Manuscript Title

Neuroprogesterone synthesis in hypothalamic astrocytes is associated with a pubertal increase in membrane ERα levels

Abbreviated Title

Estrogen signaling in astrocytes across puberty

Mohr, M.A.[1], Falcy, B.A.[1], Laham, B.J.[2], Wong, AM[1], Micevych, P.E[1]

1: UCLA DGSOM Dept of Neurobiology, 650 Charles E Young Dr. S, Los Angeles, CA 90095, Laboratory of Neuroendocrinology of the Brain Research Institute, United States of America

2:Current address: Princeton Neuroscience Institute and Department of Psychology, Princeton University, Princeton, New Jersey 085444.

Author Contributions: Each author must be identified with at least one of the following: MM and PM Designed research; MM, BF, BL, and AM performed research and analyzed data; MM, BF, and PM wrote the paper.

Correspondence should be addressed to Margaret Mohr, mmohr@mednet.ucla.edu

Acknowledgements: The authors wish to thank Carolina Thörn Perez for technical assistance during calcium imaging. This research was supported by NIH National Center for Advancing Translational Science (NCATS) UCLA CTSI grant number UL1TR001881 (MAM), and NIH Eunice Kennedy Shriver National Institute Of Child Health & Human Development grant number HD042635 (PEM).

Conflict of Interest: The authors declare no competing financial interests.

Funding sources: National Center for Advancing Translational Sciences UCLA CTSI Grant UL1TR001881 (MAM), Eunice Kennedy Shriver National Institute Of Child Health & Human Development grant number HD042635 (PEM).

ABSTRACT

The development of estrogen positive feedback is a hallmark of female puberty. Both estrogen and progesterone signaling are required for the functioning of this neuroendocrine feedback loop but the physiological changes that underlie the emergence of estrogen positive feedback remain unknown. Only after puberty does estradiol (E2) facilitate progesterone synthesis in female hypothalamic astrocytes (neuroP) (Mohr et al. 2018), an event critical for estrogen positive feedback and the LH surge. We hypothesize that prior to puberty, these astrocytes have low levels of membrane estrogen receptor alpha (ERα), making them unable to respond to E2 with increased neuroP synthesis prior to puberty. To test this hypothesis, pure populations of primary astrocyte cultures were derived from female mice at three different stages of development: pre-puberty (postnatal week 3), pubertal onset (week 5), and post-puberty (week 8). Hypothalamic astrocyte responses were measured after treatment with E2. Hypothalamic astrocytes increased progesterone synthesis across pubertal development. Prior to puberty, mERα expression was low in hypothalamic astrocytes, but expression increased across puberty. The increase in mERα expression in hypothalamic astrocytes also corresponded with an increase in caveolin-1 protein, PKA phosphorylation, and a more rapid $[Ca^{2+}]_i$ flux in response to E2. Together, these results indicate that increased mERα in hypothalamic astrocytes contributed to the post-pubertal response to E2 that results in neuroP synthesis, critical for ovulation.

SIGNIFICANCE STATEMENT

Hypothalamic astrocytes, when exposed to estradiol, make progesterone that is necessary for estrogen positive feedback during adulthood in the female rodent. However, little is known about what cellular changes occur during puberty that allow for the estradiol facilitation of progesterone synthesis. In this study, we compared cell excitability, progesterone synthesis, and levels of membrane estrogen receptor in hypothalamic astrocytes derived from pre-, mid-, and post-pubertal female mice to characterize their maturation that allows them to increase progesterone synthesis facilitating estrogen positive feedback. This study suggests that hypothalamic astrocytes acquire the necessary cellular machinery during puberty to enable E2-facilitated progesterone synthesis.

INTRODUCTION

Puberty is a complex developmental stage that elicits a barrage of neuroendocrine changes leading to reproductive maturation. In females, the development of reproductive circuits during puberty culminates in the brain responding positively to ovarian estradiol (E2), triggering the luteinizing hormone (LH) surge that underlies ovulation. There is mounting evidence that alongside E2, brain-derived progesterone (neuroP) is needed for full activation of estrogen positive feedback: 1) astrocyte-derived neuroP is crucial for fully stimulating kisspeptin release in an in vitro model of adult anterior hypothalamic kisspeptin neurons (Mittelman-Smith et al. 2015, Mittelman-Smith et al. 2018), 2) blocking neuroP synthesis arrests estrous cyclicity and decreases the LH surge (Micevych et al. 2003, Micevych et al. 2008), and 3) deleting the nuclear progesterone receptor (PGR) from kisspeptin neurons diminishes the LH surge and decreases fertility in mice (Stephens et al. 2015). What leads to the development of neuroP synthesis during puberty remains unknown.

Steroid hormones, including E2 and P4, act directly in the nucleus as well as at the membrane, initiating non-classical signaling that elicits intracellular changes that can affect transcription (Mittelman-Smith et al. 2017). E2 membrane-initiated signaling elicits elevated intracellular calcium levels and rapid P4 synthesis in hypothalamic astrocytes (Micevych et al. 2007), which are the source of neuroP. E2-facilitated neuroP synthesis in astrocytes is initiated via membrane-associated ER-alpha (mERα) transactivation of metabotropic glutamate receptor 1a (mGluR1a; (Micevych et al. 2017)). The shuttling of mERα to the plasma membrane and subsequent coupling to an mGluR subtype is regulated by a class of lipid raft proteins, called caveolins (Luoma et al. 2008). In a process necessary for neuroP synthesis, caveolin-1 shuttles full-length mERα to the plasma membrane in association with mGluR1a. E2 binding initiates excitatory downstream signaling cascades, including IP_3 receptor-dependent intracellular Ca^{2+} flux (Chaban et al. 2004) and the phosphorylation of PKA (Chen et al. 2014). Activated steroidogenic acute regulatory protein (StAR) and translocator protein (TSPO) mediate the transport of cholesterol into the mitochondria where P450scc converts it into pregnenolone. Finally, 3β-hydroxysteroid dehydrogenase (3β-HSD) converts pregnenolone into P4. Rapid E2 signaling in female hypothalamic astrocytes, eliciting intracellular Ca^{2+} flux and subsequent P4 synthesis, occurs within minutes of E2 exposure (Kuo et al. 2010).

Like the LH surge, E2-facilitated neuroP synthesis is observed solely in post-pubertal females. Indeed, astrocytes derived from the adult female hypothalamus respond to E2

stimulation with an increase in neuroP synthesis. Recently, Mohr et al. 2018, formally tested whether systemic administration of E2 to pre- and post-pubertal ovariectomized rats induced neuroP in the hypothalamus. Only post-pubertal female rats had elevated hypothalamic neuroP levels (Mohr et al. 2018). Moreover, neuroP levels were elevated on proestrus in gonadally intact female rats. Thus, in vivo and in vitro studies suggest that during puberty, hypothalamic astrocytes develop the cellular machinery to respond to E2 with neuroP synthesis. To explore this hypothesis, the present study examined neuroP synthesis, and the sequelae of E2 action in astrocytes that are associated with neuroP synthesis: E2-induced $[Ca^{2+}]_i$, levels of membrane ERα and expression of proteins associated with steroidogenesis at three specific time points in pubertal development (postnatal week 3 - pre-puberty; week 5 - pubertal onset and week 8 - post-puberty).

MATERIALS AND METHODS

All experimental procedures were performed in accordance with the principles and procedures of the National Institutes of Health Guide for the Care and Use of Laboratory Animals and approved by University of California, Los Angeles.

Primary astrocyte culture.

Primary hypothalamic astrocyte cultures were prepared from a total of 93 C57Bl/6 female mice (Jackson) consisting of 3 ages: postnatal day (PND) 23 (n = 34), 35 (n = 30), and 60 (n = 29). Cultures were generated from cohorts containing 8-12 animals (n = 4/age) at a time. In some cases where data are represented as fold change from PND 23 control, the cohort consisted of a PND 23 group with either a PND 35 or PND 60 group. Hypothalamic blocks were dissected with the following boundaries: rostral extent of the optic chiasm, rostral extent of the mammillary bodies, lateral edges of the tuber cinereum, and the top of the third ventricle. The tissue was minced, dissociated by enzymatic treatment with 2.5% trypsin solution (Invitrogen) with DNase I (Sigma #D4263) and incubated in a 37°C water bath where it was agitated every 10 min for 30 min. The trypsin was removed and 5 ml DMEM/F12 (Mediatech), supplemented with 10% fetal bovine serum (FBS) (Invitrogen), 1% penicillin (10000 IU/mL)/streptomycin (10000 µg/mL) solution (Mediatech), and 2 mM L-glutamine (Hyclone) was added. The tissue was triturated 6 times with a 5 ml pipette. Cells were plated in T-75 flasks with 10 ml DMEM/F12 (Mediatech), supplemented with 20% fetal bovine serum (FBS) (Invitrogen), 1% penicillin (10000

IU/mL)/streptomycin (10000 µg/mL) solution (Mediatech), and 2 mM L-glutamine (Hyclone) and maintained at 37°C with 5% CO2 for 3 days before the medium was replaced. After 1 week, FBS concentration was decreased to 15%. After 2 weeks, FBS concentration was decreased to 10%. Astrocyte cultures were grown to confluence and shaken on an orbital shaker at 200 rpm for 4 hours to eliminate oligodendrocytes and microglia, yielding cultures with >95% glial fibrillary acid protein-immunoreactive astrocytes. Before experimental manipulations, astrocytes were steroid- starved for 2 hours with 5% charcoal-stripped dextran-treated FBS in phenol-free DMEM/F12 medium. Cultures were then treated with vehicle dimethylsulfoxide (DMSO; Sigma-Aldrich, cat# D2650) or 17β-estradiol (1 or 10 nM; Sigma-Aldrich, cat #: E-8875) in steroid-free media (see above) for 1 hour at 37°C. After E2 treatment, media was collected for P4 analysis and cells were collected for immunoblotting.

Progesterone Extraction and ELISA.

NeuroP was extracted from conditioned astrocyte media using diethyl ether and frozen at -20°C. Frozen steroids were reconstituted in assay buffer (Cat# 80-0010). Enzo Scientific Progesterone ELISA kit (cat #ADI-900-011) was used to measure [P4], according to manufacturer's instructions. Positive (blank media spiked with 50 ng/ml P4) and negative controls (blank media alone) were run with the samples. Standard curve (R2=0.996). The detectable range of P4 was 8.57 - 500 pg/ml. Inter-assay coefficients of variation were between 2.7% and 8.3%, and intra-assay coefficients of variation were between 4.9% and 7.6%.

Calcium Imaging.

Astrocytes (375,000-570,000) were plated onto poly-d-lysine (0.1 mg/ml; Sigma-Aldrich)-coated glass coverslips and 1-2 days later pretreated for 2 h with 5% charcoal-stripped FBS DMEM/F-12 medium. Before imaging, cells were loaded with the calcium indicator Fluo 4-AM (3 µM; Thermo-Fisher; F14201) dissolved in HBSS with 0.3% DMSO and 0.06% Pluronic F-127 (Thermo-Fisher; P3000MP) for 45 min at 37°C. HBSS was used to wash the cells and then glass coverslips were mounted onto a 50-mm chamber insert (Warner Instruments) fixed into 60 x 15-mm cell culture dish (Dow Corning) and placed into a QE-2 quick exchange platform (Warner Instruments) for imaging on a Zeiss Examiner D1 microscope, using an Achroplan 20/0,50 water immersion objective (Zeiss). A perfusion pump (1 ml/min, 37°C) was used to deliver HBSS before and after application of E2 (100 pM diluted from DMSO-stocks in HBSS,

17β-estradiol, Sigma-Aldrich, cat # E-8875) or ATP (30 uM diluted in HBSS; Sigma Aldrich, cat# A2383). Fluo-4AM fluorescence was excited with the 488-nm argon laser, and emission signals above 505 nm were collected. Videos consisted of 1200 frames (512 x 512) taken, on average, every 161.08 ms (6.2 Hz, +/- 0.4 ms). Calcium flux was measured as Δ F/F, or the change in fluorescence intensity after E2 or ATP treatment over the fluorescent intensity during HBSS treatment before stimulation. Peak values were defined as the highest Δ F/F value obtained after the perfusion with E2 or ATP. Responding cells were those whose peak values were at least 20% above the baseline value prior to E2 or ATP delivery.

Cell Surface Biotinylation.

Astrocytes were pretreated for 2 h with 5% charcoal-stripped FBS DMEM/F-12 medium and incubated with DMSO vehicle or in the presence 1 nM 17-estradiol (Sigma-Aldrich) in 5% charcoal-stripped FBS DMEM/F-12 medium for 1 h at 37°C. Cells were then washed three times with ice-cold HBSS with Ca^{2+} and Mg^{2+} buffer and incubated with freshly prepared 0.5 mg/ml EZ-Link Sulfo-NHS-LC-Biotin (Pierce) in HBSS at 4°C for 30 min with gentle agitation. Excess biotin reagent was quenched by rinsing the cells three times with ice-cold glycine buffer (50 mM glycine in HBSS). Cells were scraped into 10 ml of HBSS solution, transferred into a 50 ml conical tube, and centrifuged at 850 x g for 5 min. The pellet was resuspended in 200 µl of RIPA Lysis Buffer (Santa Cruz Biotechnology) containing the following proteases inhibitors: 1 mM phenylmethylsulfonyl fluoride, 1 mM EDTA, 1 g/ml pepstatin, 1 g/ml leupeptin, 1 g/ml aprotinin, and 1 mM sodium orthovanadate (all inhibitors were from Santa Cruz Biotechnology). The cells were homogenized by passing through a 25 gauge needle 10 times every 10 min for a total of 30 min. The cell extract was centrifuged at 14,000 rpm for 5 min at 4°C, and the protein concentration of the supernatant was determined using the bicinchoninic acid (BCA) Assay (Pierce). Two hundred microliters of each sample with 1500 g/ml protein concentration was incubated with 200 µl of Immobilized NeutrAvidin Gel (Pierce) overnight at 4°C and spun for 1 min at 1000 x g. The beads were washed four times with 500 µl of radioimmunoprecipitation assay (RIPA) buffer (Santa Cruz Biotechnology) containing the same proteases inhibitors mentioned previously. The bound proteins were eluted with Laemmli Buffer containing BME (950 µl Laemmli, 50 µl of BME) for 2 h at 37°C before centrifugation at 14000 rpm for 5 min.

Immunoblotting.

For Western blotting, astrocyte cultures were washed three times with 10 mL PBS buffer and collected by mechanical scraping (Corning). The samples were centrifuged (850 x g for 5 minutes), aspirated of PBS, and lysed in RIPA lysis buffer (Santa Cruz) with protease inhibitor and phosphatase inhibitor (Invitrogen). Pellets were sonicated at 3 x 10 pulses and kept on ice for 30 min before 4°C centrifugation at 14000 x g for 5 min. Protein concentrations were determined using the BCA Assay (Pierce). Protein (10 µg of whole-cell lysates; 40 µl of surface biotinylated lysates) of each sample was loaded on an 8-16% (for TSPO, 3b-HSD, and StAR) or 4-20% (for mERα, caveolin-1, and PKA) SDS precast gels (Bio-Rad) and separated by electrophoresis. Proteins were transferred onto PVDF (GE) membranes using electrophoresis at 11 V for 18 hours (Invitrogen). Because GAPDH protein changed across puberty (data not shown) a Ponceau S (0.5% Ponceau S with 1% acetic acid) stain was done for westerns using whole-cell lysates and the 45 kDa band was imaged and used as a loading control (Olesen and Auger 2005). Membranes were probed with primary rabbit or mouse monoclonal or polyclonal antibodies diluted in 5% bovine serum albumin or nonfat dry milk in Tris-buffered saline/Tween 20 (0.1% [vol/vol]) according to the suppliers' recommendations (see Table 1). Primary incubations lasted overnight, except for ERα (3 nights) and caveolin-1 (2 nights). Blots were then incubated with goat anti-rabbit or mouse IgG horseradish peroxidase (1:10,000; Vector Laboratories) for 2 hours at room temperature. Bands were visualized using an enhanced chemiluminescence (ECL) kit (Thermo Fisher Scientific). Ponceau S (whole-cell) or Flotillin (biotinylation) was used as a loading control, and immunoreactive bands were normalized to obtain the percentage of protein to Ponceau S or Flotillin ratio. Bands were immediately visualized using FluorChem E and analyzed by Alphaview software (Cell Bioscience). To normalize the data as fold change from PND23 vehicle-treated for each target, the same PND23 vehicle-treated lysates were included across blots. Samples from similar treatment groups were pooled to achieve a minimum of 10 µg total protein per western blot lane.

Reverse Transcription Polymerase Chain Reaction (PCR).

RNA was extracted from astrocytes using TRIzol (Invitrogen) reagent, according to manufacturer's protocol. Following chloroform extraction of RNA and precipitation with 100% isopropanol, RNA pellet was washed with 75% ethanol/DEPC-treated water. RNA pellets dried for 10 min at room temperature and were re-suspended in DEPC-treated water. RNA

concentration and quality was assessed using a spectrophotometer (NanoDrop 1000). RNA was then converted to cDNA using Superscript III First Strand Synthesis Kit (Invitrogen, cat #18080-051). cDNA was made using Oligo dTs for Tspo, Esr1, and HSD3B1, and random hexamers for StAR using 1-2 µg RNA. The RT reaction was performed using a thermal cycler (Agilent Technologies, Stratagene Mx3000P) with the following parameters: for Oligo dTs, 50 min at 50°C and 5 min at 85°C; for random hexamers, 10 min at 25°C, 1 hr at 50°C, 10 min at 85°C. cDNA was used immediately for qPCR or stored at -20°C for ≤ 1 month.

See Table 2 for primer information. PCR reactions were run in duplicate (if using SYBR GreenER primers) or triplicate (if using TaqMan primers), and at least 3 duplicates/triplicates per condition were included in each PCR assay. No template controls (NTC; cDNA reverse transcribed without RNA) were run alongside cDNA for each primer pair in every PCR experiment. No amplification was observed in NTC wells. PCR reactions were prepared using 2 µL of cDNA in a 20 µL reaction with SYBR GreenER qPCR SuperMix Universal (Invitrogen; Carlsbad, CA) or Taqman Gene Expression Master Mix (Thermo Fisher, cat # 4369016). Conditions for amplification using SYBR GreenER primers were as follows: 2 min at 50°C (UDG incubation), 10 min at 95° C for UDG inactivation and DNA polymerase activation, then 50 cycles each (SYBR GreenER primers) or 40 cycles each (TaqMan primers) consisting of 15 sec at 95° C and 60 sec at the annealing temperature (60°C).

Statistics.

Data are presented as means ±SEM. Statistical comparisons were made using GraphPad Prism 7.01 Software (La Jolla, California). One-way ANOVAs were performed to determine if mRNA changes as a function of age. Two-way ANOVAs with Tukey's multiple comparisons post hoc tests were performed to determine if protein levels or P4 synthesis change as a function of age and/or estrogen treatment. Statistical significance was considered if $p \leq 0.05$.

RESULTS

P4 levels increased across puberty in female mouse hypothalamic astrocytes

After treating female mouse hypothalamic astrocytes with 10 nM E2 for 3 hrs, media was collected, steroids were extracted, and neuroP was measured to determine if P4 synthesis increases across pubertal development. Two-way ANOVA with age and hormone treatment as

independent variables and neuroP (pg/ml) as the dependent variable was performed and revealed a significant main effect of age ($F(2, 16) = 3.9$, $p = 0.0418$). Tukey post-hoc tests comparing [neuroP] at different ages indicated a nearly significant increase in P4 from PND 23 to PND 60 ($p = 0.053$). n= media from 4 T75 flasks/grp for PND23 and PND35, n = media from 3 T75 flasks/grp for PND 60.

E2-induced $[Ca^{2+}]_i$ in hypothalamic astrocytes across puberty

To determine if the response to E2 changes during pubertal development, prepubertal and adult female mouse hypothalamic astrocytes loaded with a calcium indicator (Fluo-4 AM) were treated with E2 and the change in fluorescence from baseline was monitored using epi-fluorescence. Pre-pubertal hypothalamic astrocytes exhibit both an attenuated and sustained release of intracellular calcium in response to E2 treatment, compared with the rapid and transient response of these cells after puberty (Figure 2B-D). Unpaired t-tests comparing peak delta F/F indicated that adult responses to 100 pM E2 were significantly higher than the prepubertal responses to 100 pM E2 ($t(20) = 7.517$, $p < 0.0001$; Figure 2C). Using ATP as a control for inducing intracellular calcium levels, both pre- and post-pubertal astrocytes were capable of having rapid and equally large responses, however pre-pubertal astrocytes were slower to recover, as indicated by their sustained response (Figure 2E).

Steroidogenic proteins

We did not observe any changes in steroidogenic protein expression across pubertal development. Neither levels of mRNA coding for StAR, TSPO, and 3β-HSD, nor the resulting proteins differed at the time points examined. Separate two-way ANOVAs with age and 10 nM E2 treatment as independent variables and fold change in protein (normalized to Ponceau S) from PND 23 vehicle-treated as the dependent variable was performed for StAR, TSPO, and 3β-HSD. StAR protein levels did not change across pubertal development in female mouse hypothalamic astrocytes. While age significantly affected TSPO protein levels ($F(2,34) = 4.127$, $p = 0.0249$), Tukey post-hoc tests indicated a significant decrease from pre-puberty to puberty ($p = 0.0487$), whereas prepubertal and adult female astrocytes did not differ in TSPO protein levels. E2 treatment significantly altered 3β-HSD protein levels ($F(1,33) = 4.61$, $p = 0.0392$), without any effects of age. Using Bonferroni post-hoc tests to compare the effect of E2 on 3β-HSD expression at each age separately revealed no significant differences. One-way ANOVAs

were performed with age as the independent variable and fold change in mRNA from PND23 astrocytes as the dependent variable revealed no significant differences in levels of StAR, TSPO, or 3β-HSD mRNA across pubertal development in female mouse hypothalamic astrocytes in vitro.

ERα mRNA and membrane ERα

Esr1 mRNA levels in female mouse hypothalamic astrocytes harvested from prepubertal, pubertal, and adult female mice were compared using PCR. No changes in Esr1 mRNA were detected across the time points analyzed (one-way ANOVA; $p = 0.105$; Figure 4A). Surface biotinylation and western blotting revealed that the protein levels of the full-length (66kDa) ERα changed across pubertal development but not in response to 1 nM E2 treatment (Figure 4B). Two-way ANOVA with age and hormone treatment as independent variables and fold change from P23 vehicle-treated mERα protein level as the dependent variable revealed a significant main effect of age on mERα levels ($F(2, 55) = 4.403$, $p = 0.0168$). Tukey post-hoc tests comparing mERα at different ages indicated that mERα protein concentration in female mouse hypothalamic astrocytes increased 3.1-fold from pre- to mid-puberty (1.56 ± 0.17 to 4.87 ± 1.51, $p = 0.0316$) and increased 3.2-fold from pre-puberty to adulthood (1.56 ± 0.17 to 5.02 ± 0.38, $p = 0.0264$). Mid-pubertal and adult astrocytes did not differ in mERα concentration ($p = 0.997$).

Caveolin-1 protein

Caveolin proteins are required for ER trafficking to the membrane (Meitzen and Mermelstein, 2011). Because ERα increased across development, we also examined the expression of caveolin proteins. Whole-cell lysates of E2 or vehicle treated hypothalamic astrocytes at different ages were analyzed by western blotting (Figure 5). Two-way ANOVA with age and hormone treatment as independent variables and the fold change in caveolin-1 protein (normalized to Ponceau S) from vehicle-treated PND 23 astrocytes as the dependent variable revealed a significant main effect of age ($F(2, 22) = 7.814$, $p = 0.0027$). Tukey post-hoc tests indicate a significant 3-fold increase in caveolin-1 protein from prepuberty/puberty to adulthood (PND23 < PND60, $p = 0.0064$; PND35 < PND60, $p = 0.0051$).

Phosphorylated PKA increased across puberty

We did not observe any changes in steroidogenic protein levels from prepuberty into adulthood, but there was a developmental increase in neuroP levels, suggesting that the activation of steroidogenic proteins might be increasing. Membrane ERα signaling activates PKA to phosphorylate StAR and TSPO (Chen et al. 2014) to then increase the transport of cholesterol into the mitochondrial matrix (Papadopoulos et al. 2006), the rate-limiting step of steroidogenesis. Levels of phospho-PKA from whole-astrocyte lysates were normalized to total PKA at each developmental time point (Figure 6). Two-way ANOVA, with age and hormone treatment as independent variables and the fold change in phospho-PKA/total PKA from PND 23 vehicle-treated as the dependent variable, revealed a significant main effect of age ($F(2, 43) = 5.29$, $p = 0.0088$). Tukey post-hoc tests indicate a significant ~2-fold increase in phospho-PKA/total PKA from prepuberty/puberty to adulthood (PND23 < PND60, $p = 0.0054$; PND35 < PND60, $p = 0.0167$).

DISCUSSION

The major findings of the present study are that as hypothalamic astrocytes respond to E2 with augmented neuroP synthesis across pubertal development, as the levels of mERα increased. The coordinate increase in mERα levels was associated with an increase in PKA activation and E2-induced neuroP. The current results with hypothalamic astrocytes parallel earlier results in the female rat that demonstrate neuroP synthesis increases across puberty (Mohr et al. 2018). Our current understanding of the female neuroendocrine circuit implicates neuroP in augmenting E2-induced kisspeptin expression and release. This kisspeptin in turn stimulates GnRH neurons and the released GnRH induces a LH surge. Indeed, knocking out progesterone receptor from kisspeptin neurons attenuates the LH surge (Stephens et al. 2015). Our finding suggests that post-pubertal female hypothalamic astrocytes are able to increase P4 compared with pre-pubertal female hypothalamic astrocytes. Our study aimed to further elucidate this mechanism by comparing the cellular machinery involved in neuroP synthesis in hypothalamic astrocytes harvested from female mice at different stages of pubertal development.

Both pre- and post-pubertal female mouse hypothalamic astrocytes responded to E2 administration with increased $[Ca^{2+}]_i$, however their responses are different. Prepubertal

hypothalamic astrocytes exhibited a smaller but longer-lasting E2-induced intracellular calcium release. Adult hypothalamic astrocytes, on the other hand, demonstrated a rapid, higher and more transient $[Ca^{2+}]_i$ response to E2. Additionally, the adult astrocytes responded more robustly to E2 than the pre-pubertal astrocytes. Whether these differences have functional significance remains unknown. When Kuo et al., (2010) compared $[Ca^{2+}]_i$ responses to E2 in adult male astrocytes with responses in adult female astrocytes a similar effect was observed – males had an attenuated $[Ca^{2+}]_i$ response. Moreover, male astrocytes, which synthesize a low level of neuroP, could not be stimulated by E2 to increase their neuroP synthesis. The response to E2 is similar in prepubertal female astrocytes and adult male astrocytes, further suggesting that adult female hypothalamic astrocytes undergo pubertal changes to allow them to synthesize neuroP. The present experiments revealed that only in post-pubertal astrocytes was PKA activated, which is needed for the E2 augmentation of neuroP synthesis (Chen et al. 2014). These findings suggest that intracellular signaling mechanisms in pre-pubertal astrocytes are different from those in adult females. One possibility is that mER, through which E2 signals, changes during development.

Estradiol signaling at the membrane is dependent on the mGluR transactivated by mER (reviewed in (Meitzen et al. 2017)). For E2- facilitated neuroP synthesis to occur, the mERα/mGluR1a complex is trafficked to the cell membrane by caveolin-1 (Christensen and Micevych 2012) and signals through an excitatory Gq to activate PLC and the release of Ca^{2+} from intracellular stores (Chaban et al. 2004). Conversely, inhibitory E2 signaling is mediated by mGluR2/3 activation of a Gi (Meitzen and Mermelstein 2011). Indeed, it has been shown that inhibitory E2 signaling in the hypothalamus was mediated by mGluR2/3 that was transactivated by a 52 kDa splice variant of ERα missing exon 4, the ERαΔ4 (Wong A.M., Scott A.K., Johnson C.S., Mohr M.A., Mittelman-Smith M.A., Micevych P.E, unpublished observations) . In the present study, estradiol was able to elicit an attenuated $[Ca^{2+}]_i$ in prepubertal astrocytes, perhaps due to the low-levels of full-length mERα. In these astrocytes, E2 could be signaling through an entirely different membrane-associated receptor, GPR30, whose signaling can mediate rapid E2 effects (Kuo et al. 2010). As mERα and caveolin-1 increase with development, the E2 increase in hypothalamic neuroP synthesis also increases.

We quantified mRNA and proteins levels of steroidogenic proteins to assess whether our observed developmental changes in neuroP synthesis were due to transcriptional or translational modulation. We observed that only protein levels of TSPO decreased significantly

from pre-puberty to puberty, with no change seen in response to E2 treatment. TSPO's role in steroidogenesis remains controversial, but TSPO knockouts have implicated this protein in hormone-induced steroidogenesis (Fan et al. 2015). However, the relatively weak induction of TSPO, and lack of effect on StAR or 3β-HSD suggest that the post-pubertal responsiveness to E2 is not likely attributable to up-regulation of steroidogenically relevant proteins. Given that PKA phosphorylation significantly increased post-pubertally, and that PKA phosphorylation is necessary for the phosphorylation of TSPO and StAR, we predict that TSPO and StAR phosphorylation activation should increase post-pubertally, which would increase neuroP synthesis.

In the present study, the developmental effects on hypothalamic astrocytes were stronger than the effects of E2 stimulation, suggesting that these cells undergo dramatic change during puberty. One such change was that the sensitivity to E2 that resulted in neuroP synthesis increased across pubertal development in hypothalamic astrocytes. While prepubertal astrocytes respond rapidly to E2, albeit weakly, only adult astrocytes responded robustly and rapidly to E2 that resulted in PKA phosphorylation and neuroP synthesis. When neuroP is measured in hypothalamic tissue, either in gonadectomized and EB-replaced or gonad-intact rats, E2-facilitated P4 synthesis occurred only post-pubertally (Mohr et al. 2018), and could be explained by the presence of ERα on the membrane only after puberty in hypothalamic astrocytes.

Conclusion

In the present study hypothalamic astrocytes harvested from female mice at different ages were used to compare estradiol responsiveness across pubertal development. The response to E2 in prepubertal hypothalamic astrocytes resulted in $[Ca^{2+}]_i$ increase but due to low amounts of full-length mERα, PKA was not phosphorylated and P4 synthesis remained low. The response to E2 in post-pubertal hypothalamic astrocytes was rapid, resulting in $[Ca^{2+}]_i$ flux mediated by full-length mERα, which led to PKA phosphorylation and neuroP synthesis. The expression of full-length mERα after puberty in hypothalamic astrocytes likely underlies the female's distinctly post-pubertal response to E2 to produce neuroP, which is critical for ovulation.

References

Chaban, V. V., A. J. Lakhter and P. Micevych (2004). "A membrane estrogen receptor mediates intracellular calcium release in astrocytes." Endocrinology **145**(8): 3788-3795.

Chen, C., J. Kuo, A. Wong and P. Micevych (2014). "Estradiol Modulates Translocator Protein (TSPO) and Steroid Acute Regulatory Protein (StAR) via Protein Kinase A (PKA) signaling in Hypothalamic Astrocytes." Endocrinology **155**(8): 2976-2985.

Christensen, A. and P. Micevych (2012). "CAV1 siRNA reduces membrane estrogen receptor-alpha levels and attenuates sexual receptivity." Endocrinology **153**(8): 3872-3877.

Fan, J., E. Campioli, A. Midzak, M. Culty and V. Papadopoulos (2015). "Conditional steroidogenic cell-targeted deletion of TSPO unveils a crucial role in viability and hormone-dependent steroid formation." Proceedings of the National Academy of Sciences **112**(23): 7261.

Kuo, J., N. Hamid, G. Bondar, E. R. Prossnitz and P. Micevych (2010). "Membrane estrogen receptors stimulate intracellular calcium release and progesterone synthesis in hypothalamic astrocytes." Journal of Neuroscience **30**(39): 12950-12957.

Luoma, J. I., M. I. Boulware and P. G. Mermelstein (2008). "Caveolin proteins and estrogen signaling in the brain." Molecular and cellular endocrinology **290**(1-2): 8-13.

Meitzen, J., K. A. Britson, K. Tuomela and P. G. Mermelstein (2017). "The expression of select genes necessary for membrane-associated estrogen receptor signaling differ by sex in adult rat hippocampus." Steroids.

Meitzen, J. and P. G. Mermelstein (2011). "Estrogen receptors stimulate brain region specific metabotropic glutamate receptors to rapidly initiate signal transduction pathways." J Chem Neuroanat **42**(4): 236-241.

Micevych, P., K. Sinchak, R. H. Mills, L. Tao, P. LaPolt and J. K. Lu (2003). "The luteinizing hormone surge is preceded by an estrogen-induced increase of hypothalamic progesterone in ovariectomized and adrenalectomized rats." Neuroendocrinology **78**(1): 29-35.

Micevych, P., K. K. Soma and K. Sinchak (2008). "Neuroprogesterone: Key to estrogen positive feedback?" Brain Res Rev **57**(2): 470-480.

Micevych, P. E., V. Chaban, J. Ogi, P. Dewing, J. K. Lu and K. Sinchak (2007). "Estradiol stimulates progesterone synthesis in hypothalamic astrocyte cultures." Endocrinology **148**(2): 782-789.

Micevych, P. E., P. G. Mermelstein and K. Sinchak (2017). "Estradiol Membrane-Initiated Signaling in the Brain Mediates Reproduction." Trends Neurosci **40**(11): 654-666.

Mittelman-Smith, M. A., L. M. Rudolph, M. A. Mohr and P. E. Micevych (2017). "Rodent Models of Non-classical Progesterone Action Regulating Ovulation." Front Endocrinol (Lausanne) **8**: 165.

Mittelman-Smith, M. A., A. M. Wong, A. S. Kathiresan and P. E. Micevych (2015). "Classical and membrane-initiated estrogen signaling in an in vitro model of anterior hypothalamic kisspeptin neurons." Endocrinology **156**(6): 2162-2173.

Mittelman-Smith, M. A., A. M. Wong and P. E. Micevych (2018). "Estrogen and Progesterone Integration in an in vitro Model of RP3V Kisspeptin Neurons." Neuroendocrinology **106**(2): 101-115.

Mohr, M. A., A. M. Wong, R. J. Tomm, K. K. Soma and P. E. Micevych (2018). "Pubertal development of estradiol-induced hypothalamic progesterone synthesis." Horm Behav.

Olesen, K. M. and A. P. Auger (2005). "Sex differences in Fos protein expression in the neonatal rat brain." J Neuroendocrinol **17**(4): 255-261.

Papadopoulos, V., M. Baraldi, T. R. Guilarte, T. B. Knudsen, J. J. Lacapere, P. Lindemann, M. D. Norenberg, D. Nutt, A. Weizman, M. R. Zhang and M. Gavish (2006). "Translocator protein (18kDa): new nomenclature for the peripheral-type benzodiazepine receptor based on its structure and molecular function." Trends in pharmacological sciences **27**(8): 402-409.

Stephens, S. B., K. P. Tolson, M. L. Rouse, Jr., M. C. Poling, M. K. Hashimoto-Partyka, P. L. Mellon and A. S. Kauffman (2015). "Absent Progesterone Signaling in Kisspeptin Neurons Disrupts the LH Surge and Impairs Fertility in Female Mice." Endocrinology **156**(9): 3091-3097.

Figure Legends

Figure 1. E2-facilitated P4 synthesis increases in female mouse hypothalamic astrocytes across puberty. Hypothalamic astrocytes harvested from 60 day-old female mice synthesized significantly more progesterone compared with astrocytes harvested from 23 day-old female mice after 10 nM E2 treatment for 3 hrs. Data indicate the amount of progesterone (pg/ml) present in the media of astrocytes harvested from female mice at different stages of pubertal development ± SEM. n = 3-4/group. * $p < 0.05$.

Figure 2. Prepubertal and adult astrocytes respond differently to E2. A) Representative image of a hypothalamic astrocyte loaded with calcium indicator Fluo-4 AM. Scale bar = 10 µm. B) Representative traces of $[Ca^{2+}]_i$ in hypothalamic astrocytes harvested from postnatal day 23 (prepubertal) or 60 (adult) female mice loaded with Fluo-4 AM and treated with 100 pM E2. C) An unpaired t-test comparing the average peak in fluorescence indicated that adult astrocytes treated with 100 pM E2 elicited the most $[Ca^{2+}]_i$ compared with the prepubertal astrocytes. D) Percentage of astrocytes not responding to E2 (p delta F/F < 1.2), responding with a delay (p delta F/F > 1.2 occurring after 50 sec), and responding rapidly (p delta F/F > 1.2 occurring within 50 sec of E2 application). E) Prepubertal and adult astrocytes exhibited a robust $[Ca^{2+}]_i$ flux when treated with 30 µM ATP. An unpaired t-test indicated no difference in peak delta F/F between prepubertal and adult astrocytes ($p = 0.087$). Dotted lines indicate baseline fluorescence. Sample size (n) for each condition is indicated inside bars. **** $p < 0.0001$.

Figure 3. Steroidogenic proteins were unremarkable in hypothalamic astrocytes harvested from female mice at different stages of pubertal development. Protein and mRNA levels of StAR, TSPO, and 3β-HSD remained relatively stable in hypothalamic astrocytes across pubertal development. A) StAR protein, regardless of age or E2 treatment, did not change across puberty in hypothalamic whole-astrocyte lysates. B) TSPO protein decreased from pre-puberty to puberty, with adult levels intermediate in female mouse hypothalamic astrocytes. C) Regardless of age, E2 treatment increased levels of 3β-HSD protein in female mouse hypothalamic astrocytes. D-F) StAR, TSPO, and 3β-HSD mRNA levels did not change in hypothalamic astrocytes harvested from prepubertal, pubertal, or adult female mice. Data are represented as fold change in protein (normalized to Ponceau S) or mRNA (2^-ddCt) from postnatal day 23 vehicle-treated hypothalamic astrocytes ± SEM. Sample size (n) for each condition is indicated within bars.

Figure 4. Esr1 mRNA levels were stable while mERα increased across pubertal development in female mouse hypothalamic astrocytes.

A) ERα (Esr1) mRNA did not differ in hypothalamic astrocytes taken from female mice pre, during, or post-puberty. n = RNA from individual T75 flasks, indicated within bars. B) Independent of E2-treatment, pubertal development significantly altered membrane ERα protein levels in surface biotinylated female mouse hypothalamic astrocytes. Full-length mERα levels increased after puberty in surface biotinylated lysates taken from female mouse hypothalamic astrocytes (ME of age, $p = 0.0168$). Tukey post-hoc tests indicated a significant increase in mERα from pre-puberty to mid-puberty ($p = 0.0316$) and from pre-puberty to adulthood ($p = 0.0264$). Data are plotted as fold change from P23 vehicle mERα normalized to flotillin ± SEM. *$p < 0.05$.

Figure 5. Caveolin-1 protein increased in adulthood in female mouse hypothalamic astrocytes. Independent of E2-treatment, caveolin-1 protein levels significantly increased after puberty in whole-cell lysates taken from female mouse hypothalamic astrocytes (ME of age, $p = 0.003$). Data are plotted as fold change in caveolin-1 protein from P23 vehicle-treated ± SEM. $^{**}p < 0.01$. Sample size (n) for each condition is indicated within bars.

Figure 6. PKA phosphorylation increased across puberty in female mouse hypothalamic astrocytes. Independent of E2-treatment, levels of phosphorylated PKA protein significantly increased after puberty in whole-cell lysates taken from female mouse hypothalamic astrocytes (ME of age, $p = 0.0088$). Data are plotted as fold change in phosphorylated PKA/total PKA protein from P23 vehicle-treated ± SEM. $^{**}p < 0.01$. $^{*}p < 0.05$. Sample size (n) for each condition is indicated within bars.

Figure 1

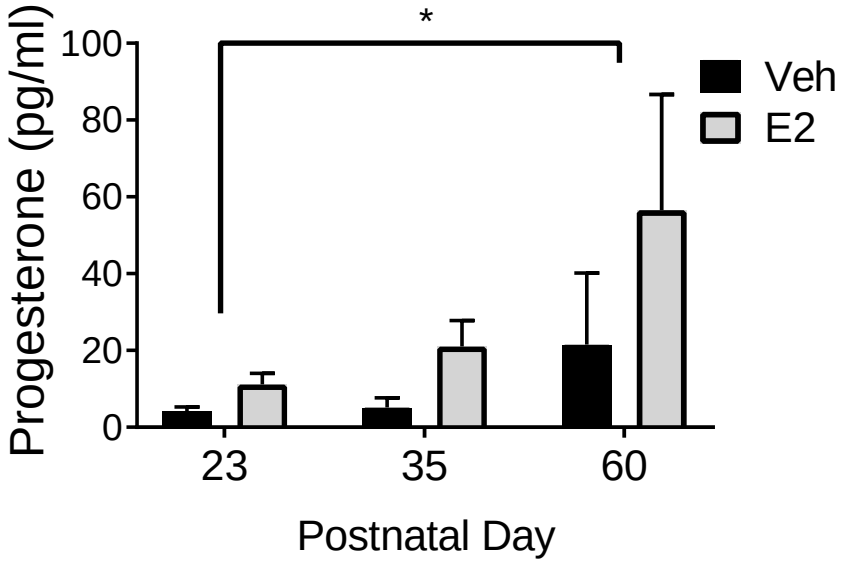
*
Progesterone (pg/ml)
100
80
60
40
20
0
23
35
60
Postnatal Day
Veh
E2

Figure 2

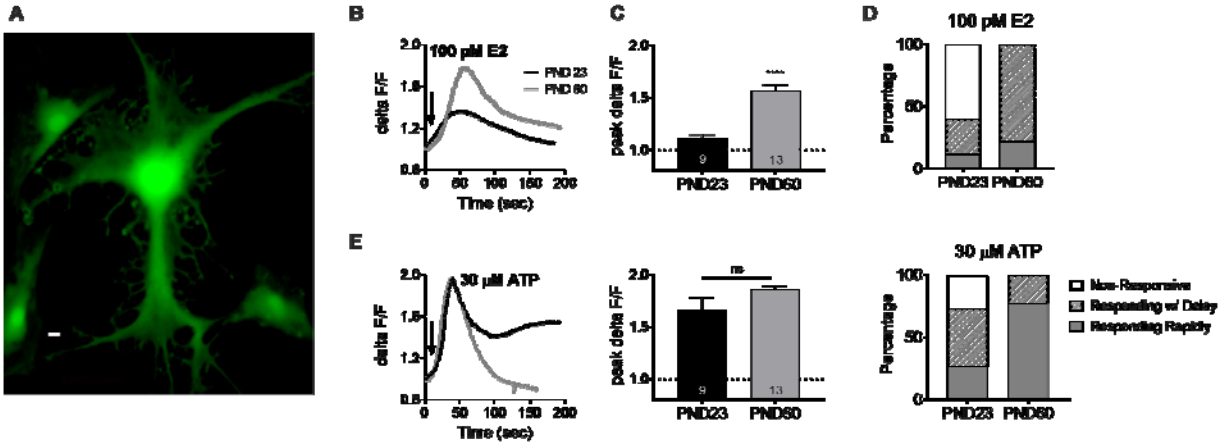
A
B
100 pM E2
PND 23
PND 60
delta F/F
Time (sec)
C
peak delta F/F
PND23
PND60
D
100 pM E2
Percentage
PND23 PND60
E
30 µM ATP
delta F/F
Time (sec)
peak delta F/F
ns
PND23
PND60
30 µM ATP
Percentage
Non-Responsive
Responding w/ Delay
Responding Rapidly
PND23 PND60

Figure 3

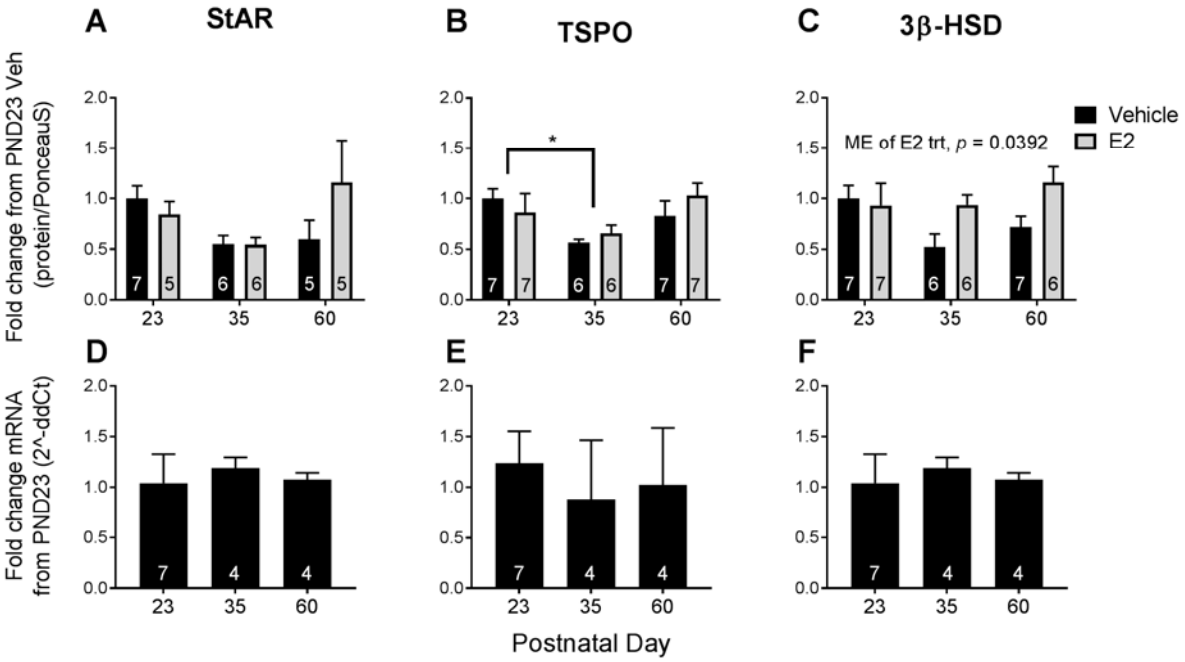
A
StAR
B
TSPO
C
3β-HSD
Fold change from PND23 Veh (protein/PonceauS)
Vehicle
E2
ME of E2 trt, p = 0.0392
*
D
E
F
Fold change mRNA from PND23 (2^-ddCt)
Postnatal Day
23
35
60

Figure 4

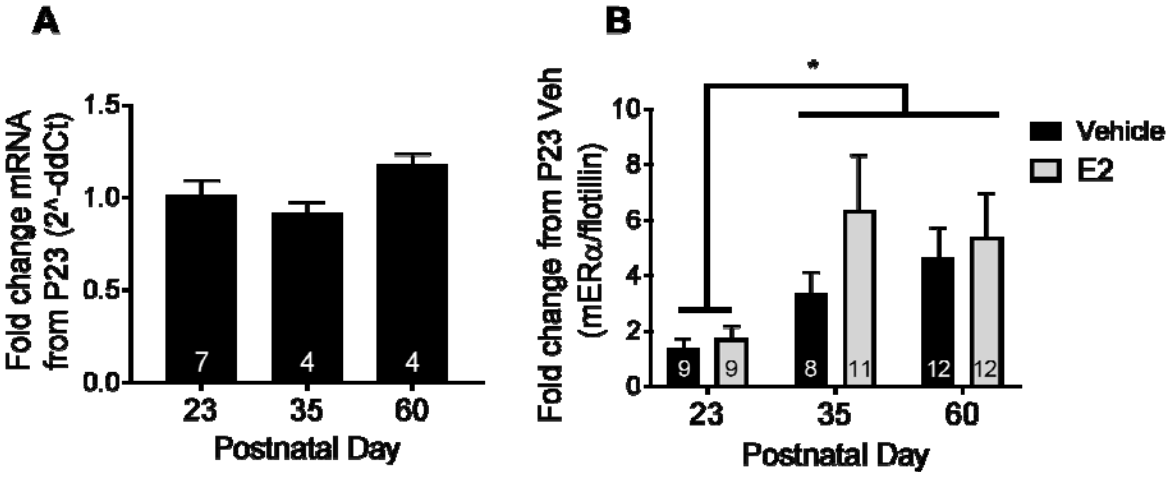
A
Fold change mRNA from P23 (2^-ddCt)
1.5
1.0
0.5
0.0
7
4
4
23
35
60
Postnatal Day
B
Fold change from P23 Veh (mERα/flotillin)
*
10
8
6
4
2
0
9
9
8
11
12
12
23
35
60
Postnatal Day
Vehicle
E2

Figure 5

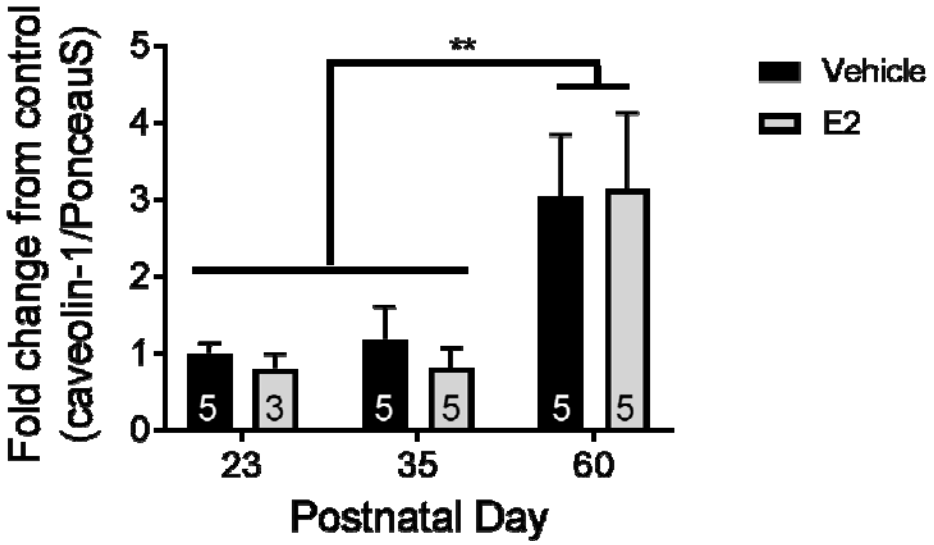
Fold change from control
(caveolin-1/PonceauS)
5
4
3
2
1
0
**
5
3
5
5
5
5
23
35
60
Postnatal Day
Vehicle
E2

Figure 6

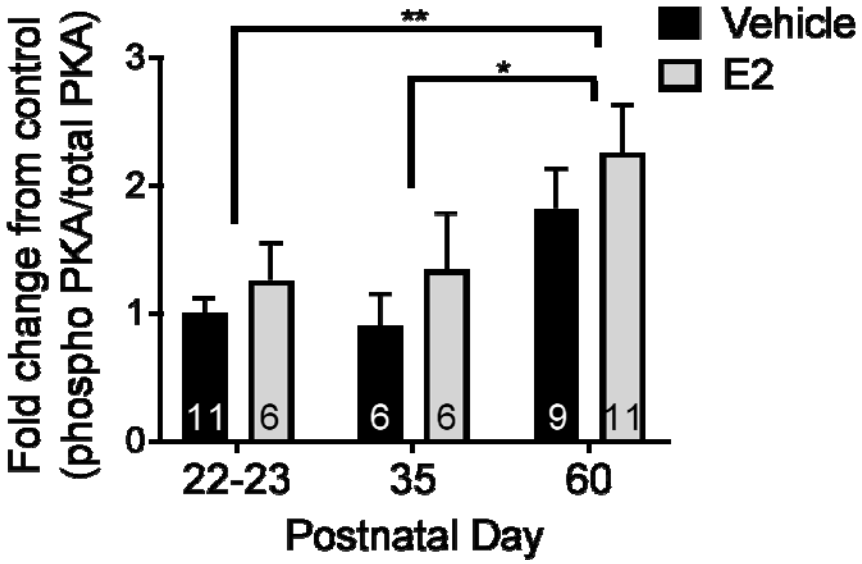
Vehicle
E2
**
*
Fold change from control
(phospho PKA/total PKA)
3
2
1
0
11
6
6
6
9
11
22-23
35
60
Postnatal Day

TABLES

Table 1. Antibody information

Antibody	Manufacturer	Catalog Number	RRID	Dilution
Rabbit monoclonal anti-3βHSD	Abcam	ab150384	n/a	1:500 in 5% milk
Mouse monoclonal anti-Caveolin 1	BD Laboratories	610407	AB_397789	1:1,000 in 5% milk
Rabbit polyclonal anti-ERα (C1355)	Millipore	06-935	AB_310305	1:1,000 in 5% BSA
Rabbit polyclonal anti-Flotillin 1	Abcam	ab41927	AB_941621	1:1,000 in 5% BSA
Goat anti-Mouse HRP	Invitrogen	A16072	AB_2534745	1:10,000 in 5% milk
Goat anti-Rabbit HRP	Invitrogen	A16104	AB_2534776	1:10,000 in 5% milk
Rabbit monoclonal anti-P-PKA C	Cell Signaling	5661	AB_10707163	1:1,000 in 5% BSA
Rabbit polyclonal anti-PKA C-α	Cell Signaling	4782	AB_2170170	1:1,000 in 5% BSA
Rabbit polyclonal anti-StAR	Abcam	ab96637	AB_10678397	1:1,000 in 5% milk
Rabbit polyclonal anti-TSPO	Cell Signaling	9530	n/a	1:1,000 in 5% BSA

Table 2. PCR Primer Information

Primer	Gene Accession #	FW Primer	RV Primer	Amplicon Size (BP)	Annealing Temperature	Ref/Assay #
Hsd3b1 (SYBR Green)	NM_008293	TGG ACA AGG TAT TCC GAC CAG A	GGC ACA CTT GCT TGA ACA CAG	250	60°C	Sarraj et al., 2010
Esr1 (SYBR Green)	NM_007956	TGG GCT TAT TGA CCA ACC TAG CA	AGA ATC TCC AGC CAG GCA CAC	130	60°C	n/a Li et al., 2013
GAPDH (SYBR Green)	NM_017008	GCA CAG TCA AGG CCG AGA AT	GCC TTC TCC ATG GTG GTG AA	150	60°C	n/a Chen et al., 2006
StAR (Taqman)	NM_011485	Exon 6	Exon 7	73	60°C	Mm00441558_m1
Tspo (Taqman)	NM_009775	Exon 3	Exon 4	116	60°C	Mm00437828_m1
GAPDH (Taqman)	NM_008084	Exon 2	Exon 3	107	60°C	4352339E